# Sub-Nano World in Steels Clarified with Cs-Corrected STEM†

YAMADA Katsumi[*1] NAKAMICHI Haruo[*2] SATO Kaoru[*3]

***Abstract:***

*More than a decade has already passed since Cs-corrected scanning electron microscope (Cs-corrected STEM) technology was launched into the electron microscopy market in 2005. JFE Steel recognized the importance of this new technology from its early stage, and in 2006 was the first in the field of steel research to install a Cs-corrected STEM, focusing on its potential as an absolutely necessary instrument for sub-nano analysis. Since 2006, JFE Steel has applied Cs-corrected STEM to the study of nano-sized MC (M: Metallic elements, C: Carbon) carbides in high strength steels, ultra-thin passive films formed on type 304 stainless steels and grain boundary segregation in Fe and Ni based alloys. Elemental analyses with sub-nanometer resolution by the Cs-corrected STEM have provided necessary and sufficient compositional information for considering fine precipitation behavior and corrosion resistance corresponding to each material.*

## 1. Introduction

The transmission electron microscope (TEM) is a key analytical technique which has driven structural characterization of materials in the nanometer region. As early as the 1960s, the image resolution of conventional TEM had already achieved 0.2 nm[1]. At the beginning of the 1990s, its spatial resolution in elemental analysis was dramatically improved by adoption of a field emission source (FE) as a high brightness electron source. JFE Steel introduced the first FE-TEM in 1990 and applied this instrument to structural characterization of the microstructures of steel materials in the nanometer region[2]. However, with market-based FE-TEM, it was not possible to obtain an adequate current value even if the electron beam could be focused to the sub-nanometer size, and in many cases, it was difficult to achieve sub-nanometer resolution in elemental analysis. This problem was overcome by the Cs-aberration correcting system for electron microscopes, which was developed by the Rose and Haider group in Germany and announced in 1998 [3]. The development of this technology made it possible to perform image observation and elemental analysis with sub-nanometer resolution with commercially-available instruments having accelerating voltages of 200–300 kV. JFE Steel was one of the first companies to recognize the importance of this technology, which was launched into the market in 2005. In 2006, JFE introduced Japan's first Cs-corrected STEM (TITAN 80–300, manufactured by FEI) ; this was also the world's first introduction of Cs-corrected STEM technology in the steel industry[4]. Since 2006, this instrument has been actively used in sub-nanometer characterization analysis of the microstructures of various steel materials. This paper presents examples of that analytical research.

## 2. Analysis of Nanometer-sized Carbides in Steel

### 2.1 Atomic Resolution STEM Image Observation

Tensile strength of 780 MPa class high strength hot-rolled steel sheet, Nano-HITEN®[5], which JFE Steel developed in 2001 is an ideal steel sheet which satisfies

† Originally published in *JFE GIHO* No. 37 (Feb. 2016), p. 11–15

[*1] Dr. Eng.,
Senior Researcher Deputy General Manager,
Analysis & Characterization Research Dept.,
Steel Res. Lab.,
JFE Steel

[*2] Dr. Eng.,
Senior Researcher Deputy General Manager,
Analysis & Characterization Research Dept.,
Steel Res. Lab.,
JFE Steel

[*3] Ph. D.,
Fellow,
Corporate Planning Dept.
JFE Techno-Research

both high tensile strength and an excellent hole expansion property. Its high formability has made an important contribution to weight saving in car bodies by application to automobile underbody parts. The fact that the main strengthening mechanism of this steel is dispersion strengthening by nanometer-sized carbides of the MC type (M: Metallic elements, C: Carbon) which are finely dispersed in soft crystal grains of ferrite, and these are realized mainly by an inter-phase precipitation phenomenon accompanying the $\gamma \rightarrow \alpha$ transformation during the coiling process in hot rolling has already been clarified[6,7]. Although active research on inter-phase precipitation was carried out at the laboratory level until the 1980s[8,9], advanced manufacturing technology is necessary to realize this phenomenon stably in an industrial operation. On the other hand, there are limits to the elucidation of the state of carbides with a size on the order of a few nanometers with conventional analytical electron microscopes, and in particular, the internal structure of those carbides is unknown. **Photo 1** shows a high resolution TEM (high resolution transmission electron microscopy, HRTEM) image of an MC type carbide consisting of Ti and Mo[10]. Although this is an HRTEM image without Cs-aberration correction, the image quality is extremely good because the installation environment is overwhelmingly superior to conventional environments, in that the instrument is installed on an active anti-vibration table, etc. This carbide is precipitated in a platelet form while basically maintaining the Baker-Nutting orientation relationship[11] with the ferrite matrix, and its growth direction is parallel to a facet plane with good crystallography coherence. **Photo 2** shows an example of atomic-level observation of a carbide by Cs-corrected STEM. This photograph is a STEM-bright field image in which an ultra-thin platelet-shaped carbide with a thickness of < 1 nm is observed from the cross-sectional direction of thickness. The facet plane of the precipitate is linear, and almost no disorder of the

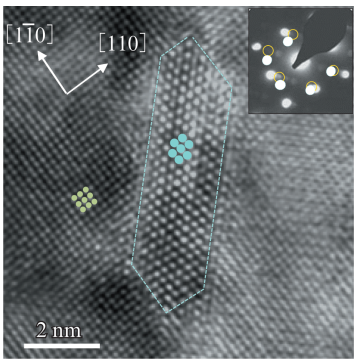


Photo 1 High resolution transmission electron microscopy (HRTEM) image of nanometer-sized MC (M: Metallic elements, C: Carbon) and its electron diffraction pattern

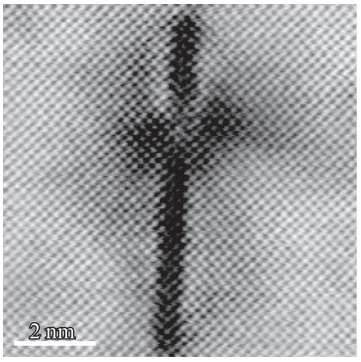


Photo 2 High resolution scanning transmission electron microscopy (HRSTEM)-bright field (BF) image of a thin platelet MC (M: Metallic elements, C: Carbon)

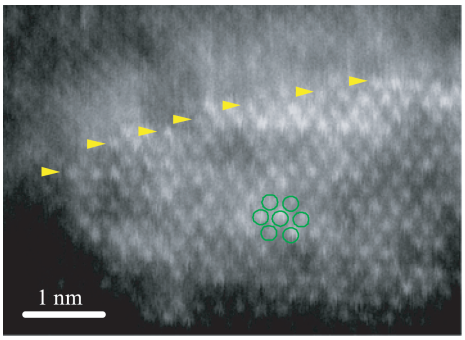


Photo 3 Cross-sectional High resolution scanning transmission electron microscopy (HRSTEM)-annular dark field (ADF) image of platelet MC (M: Metallic elements, C: Carbon)

atomic column on the matrix side can be observed. In contrast, when precipitates were intentionally coarsened by performing post heat treatment, observation revealed that this facet plane forms a step structure with an atomic plane, resulting in arc-like bulging, as shown in the high resolution STEM annular dark field (HRSTEM-ADF) image in **Photo 3**.

### 2.2 Determination of Carbide Composition by High Resolution EDS Analysis

The composition of nanometer-sized carbides discussed in section 2.1 has already been analyzed by the conventional FE-STEM method, and the ratio of the metallic elements that comprise these carbides has been clarified[7]. However, in explaining why carbides does not grow easily in the coiling process, in addition to crystallographic coherency with the matrix, it was necessary to verify with high resolution whether a retardation effect of diffusion of Mo, which is one of the elements that make up carbides, exists or not. **Photo 4** shows the result of EDS (energy dispersive X-ray spectroscopy) line analysis with an interval close to the atomic plane unit by Cs-corrected STEM.

The probe diameter during elemental analysis is less than 0.2 nm, and the interval of the line analysis across

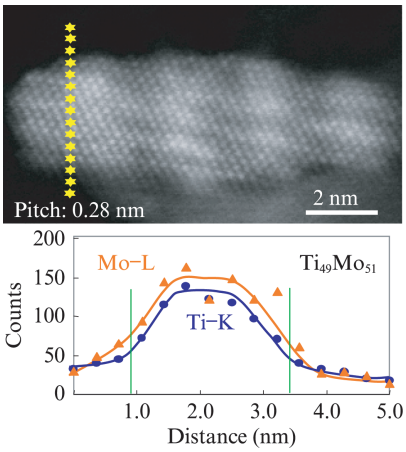


Photo 4 High resolution scanning transmission electron microscopy (HRSTEM)-annular dark field (ADF) image and its energy dispersive X-ray spectroscopy (EDS) line analysis across a platelet MC (M: Metallic elements, C: Carbon)

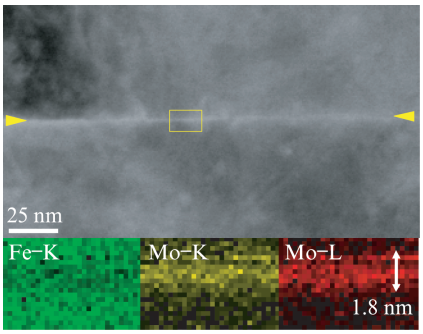


Photo 5 Scanning transmission electron microscopy (STEM)-annular dark field (ADF) image of a prior austenite grain boundary in 0.6 at% Mo bainitic steel and its energy dispersive X-ray spectroscopy (EDS) mapping that indicates Mo segregation

the thickness direction of the carbide platelet is 0.28 nm. The X-ray intensities of the metallic elements Ti and Mo which comprise the complex carbide were uniform at the periphery and in the interior of the carbide, and a condition in which Mo was diffusion-limited and Mo concentrated locally at the surface could not be observed. Based on these facts, the composition in the carbides has already become basically constant in the stage when carbides are a few nanometers in size, and the factor which suppresses their growth is considered to be exclusively crystallographic constraints, and depletion of Ti, C and other constituent elements of carbides in the coiling temperature region. Thus, it was possible to obtain fundamental composition design guidelines for the use of nanometer-sized carbides.

## 3. Sub-Nanometer Analysis at Grain Boundaries

### 3.1 Grain Boundary Segregation of Mo in Ultra-Low Carbon Bainitic Steel

Segregation of specific elements at grain boundaries has a strong influence on formation of the internal structure, intergranular embrittlement, and furthermore, on stress corrosion cracking, and thus is one key structural factor that controls material properties. For example, elements such as P and S tend to segregate to grain boundaries and easily cause intergranular cracking. For this phenomenon, intergranular fracture surface was analyzed by using the Auger electron spectroscopy (AES) to evaluate the amount of segregation and segregation width[12,13]. The effects of segregation of trace amounts of B to grain boundaries in retardation of the $\gamma \rightarrow \alpha$ transformation and suppression of anti-embrittlement in secondary work in ultra-low carbon steel sheets are widely known. However, this does not mean that cracking always occurs at those grain boundaries in the AES instrument; rather, in cases where the grain boundary is strengthened by segregation, application of fracture surface analysis is difficult. Although secondary ion mass spectroscopy (SIMS) is known as a high sensitivity analysis method for B, its spatial resolution in elemental analysis is not adequate. Due to the insufficient sensitivity of EDS, research in the TEM field is limited to EELS (electron energy loss spectroscopy)[14], and recently, Cs-corrected STEM-EELS has been used in quantitative discussions of grain boundary segregation[15].

In addition to elements such as B which have a decisive effect on the grain boundary structure when added in trace amounts, the grain boundary segregation behaviors of heavy metal elements are also important, and EDS is advantageous to Cr, Mn, Cu, Mo, etc. **Photo 5** shows the result of EDS mapping of the vicinity of the prior $\gamma$ grain boundary in an ultra-low carbon bainitic steel with 0.6 at% addition of Mo.

In quantitative analysis of grain boundary segregation of impurities, the segregation width of those elements is on the atomic plane order. Therefore, it is essential to perform the analysis under the edge-on condition, in which the incident direction of the electron beam and the grain boundary are substantially parallel. Photo 5 showed a result when observation was performed under this condition, and revealed that Mo concentrated to a maximum of approximately 1.6 at% with a width of < 2.0 nm. By conversion to the {110} crystal plane, this segregation occurs in a width of within 10 atomic layers. In the past, it was reported that Mo segregation at the grain boundary in recrystallization of ferritic steel occurred due to the solute drag effect[16]. The results described here are thought to suggest an analogous effect in the austenitic region. This is a phenomenon which should be considered based on an understand-

ing of microstructure formation in advanced steels, in which addition of various elements is intended.

It may also be noted that the fact that it has become possible to take samples for analyses from specific grain boundaries by a focused ion beam (FIB) instrument has made a major contribution to the progress of research on grain boundary segregation by TEM or STEM.

### 3.2 Segregation of Elements to Grain Boundaries in Ni-based Alloy

Regarding sensitization of high alloy steels such as stainless steels, etc., it is widely known that the formation of a Cr depletion zone accompanying carbide precipitation at grain boundaries is a prime factor in stress corrosion cracking. From around the 1990s, energy selective transmission electron microscopy and the energy-filtering TEM were applied to this phenomenon, and quantitative evaluations of the Cr depletion zone near the grain boundary were carried out[17,18]. However, selective corrosion of grain boundaries is sometimes observed in high Ni 625 alloy (Huey test: evaluation by dipping in boiling 65% nitric acid), even though no obvious grain boundary precipitation occurred. In order to clarify this phenomenon, Cs-corrected STEM was applied to a grain boundary analysis of this alloy, and as a result, enrichment of Mo and Nb on the grain boundaries and depletion of Cr were confirmed in material in which intergranular corrosion tended to occur, as shown in **Photo 6**. That compositional change was on the order of the half maximum full-width, 5 nm. Since the grain boundary composition was clearly different from that of the matrix, its sensitivity to corrosion is also thought to have been different. Although Mo is generally considered to accelerate passivation and thereby improve corrosion resistance, based on the results described here and electrochemical consideration, it is interpreted that the grain boundary in this material became an excess passivation region due to excessive segregation of Mo[19].

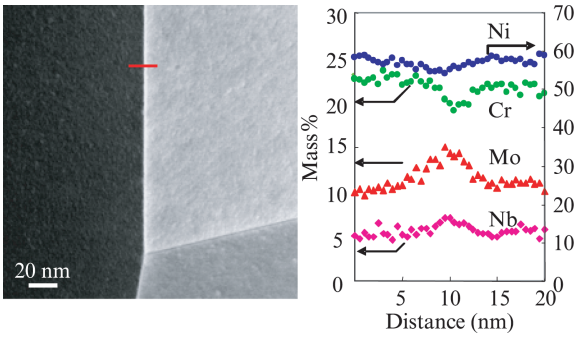


Photo 6 Scanning transmission electron microscopy (STEM) -annular dark field (ADF) image at grain boundaries in a 625 alloy and its energy dispersive X-ray spectroscopy (EDS) line analysis across a grain boundary indicated in the image

## 4. Analysis of Top Surface Passivation Film of Steel Sheets

The excellent corrosion resistance of stainless steel is known to be due to the formation of a stable passivation film with a thickness of a few nanometers on the steel sheet surface. In the past, analyses of the passivation film was performed by using apparatuses for surface analysis such as X-ray photoelectron spectroscopy (XPS), Auger electron spectroscopy (AES), etc., which yielded much knowledge concerning the composition and interfacial structure of the film[20]. However, in the AES depth profile analysis, compositional mixing at the interface caused by Ar ion sputtering was a constant concern. Moreover, because XPS has low in-plane spatial resolution, information was averaged, and it was not possible to obtain the same precision with practical steel sheets as with Si substrates and other smooth specimens.

JFE Steel applied the Cs-corrected STEM to this extremely thin film and succeeded in direct observation and elemental analysis from the cross-sectional direction. **Photo 7** shows a STEM high angle annular dark field (HAADF) image and the results of EDS elemental mapping of a region $7 \times 15\ nm^2$ of SUS304, which includes the passive film formed on the specimen. This specimen was also prepared by FIB technique. In the STEM-HAADF image at the left, the film portion appears darker than the substrate steel, and the effect of the averaged atomic number is apparent. In the results of elemental mapping in the four sections to the right, in addition to local concentration of Cr in the bottom layer of the passive film, local concentration of Ni to about 2 nm in the surface layer of the substrate steel sheet could also be observed. From the results of determination by a separate line analysis, local concentration of Cr reached a maximum of 20 mass% or more, while local concentration of Ni reached 18 mass%, which is more than two times the Ni content of the matrix[21,22]. The details of the local concentration of specific elements at the surface of the substrate steel sheet and compositional fluctuations in the interior of the extremely thin passive

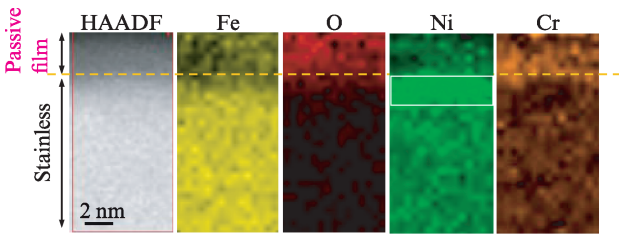


Photo 7 Cross sectional scanning transmission electron microscopy (STEM)-annular dark field (ADF) image and its energy dispersive X-ray spectroscopy (EDS) elemental mapping of a passive film formed on type 304 stainless steel

film could be obtained with higher resolution in the depth profile than was possible with AES or XPS. In the Ni-, Mo-free ferritic stainless steel JFE443 CT with excellent corrosion resistance developed by JFE Steel[23], local concentration of Cu in the surface layer of the steel was also detected, revealing the mechanism of rust prevention by Cu[24]. In this way, elemental information with sub-nanometer resolution obtained by Cs-corrected STEM is critical for understanding the passivation behavior in stainless steel. It was found that this technology is effective for elucidating the various types of surface reactions which occur within several nm of the steel sheet surface.

## 5. Conclusion

Recognizing that Cs-corrected STEM would be an essential instrument for developing the high performance steel products of the future, JFE Steel introduced a Cs-corrected STEM in 2006. This paper has presented examples of characterization of the fine structures of steel which influence mechanical, corrosion and surface properties, including carbides, the top surface layer of steel sheets, the grain boundary, etc., by sub-nanometer resolution STEM observation and EDS analysis. Actually, in order to acquire data related to the structure and composition of regions of sub-nanometer size or less, advanced specimen preparation methods are indispensable. For example, because ferritic steel materials have strong magnetism, it is difficult to perform beam alignment to obtain an electron probe with high brightness having a size of $< 0.2$ nm$\varphi$ when using Cs-corrected STEM. In FIB specimens, which were used in top surface layer analysis and grain boundary analysis, those small volume of the specimen reduced this magnetism of the specimen. However, when structural changes at the further atomic level are required, it might be necessary to reduce the specimen damage induced by the ion beam in FIB fabrication.

Although the high current density of Cs-corrected STEM is advantageous to detection of trace elements in elemental analysis, in some cases the specimen being analyzed cannot withstand electron beam irradiation. To perform high resolution measurement while also avoiding specimen damage by the electron beam during analysis, it is important to optimize the specimen thickness, probe current, dwell time per point, and also the interval between analysis points.

In spite of the issues mentioned above, it is extremely significant that observation with high resolution and elemental analysis with sub-nanometer spatial resolution are possible with steel materials by utilizing electron microscopes with an accelerating voltage of 200–300 kV. Moreover, considerable improvements have been achieved in image simulation techniques using theoretical calculations, and in EDS and EELS techniques, and it is thought that these techniques are finally entering the stage of use for practical steel research. JFE Steel will actively utilize these techniques to accelerate the development of high performance steel products in the future, and also plans to develop further advanced techniques in Cs-corrected STEM.

## References


1) Harada, Y.; Tomita, M. KENBIKYO. 2011, vol. 46, Suppl. 3, 3.
2) Yamada, K. et al. JFE Giho. 2006, no. 13, p. 18–24.
3) Haider, M.; Rose, H. Nature. 1998, vol. 392, p. 768–769.
4) Press release in Japan Metal Daily (Tekko Shimbun) and THE NIKKAN KOGYO SHIMBUN etc. on 7th. Mar. 2007.
5) Seto, K. et al. JFE Giho, 2007, no. 16, p. 28–33.
6) Funakawa, Y. et al. ISIJ Int. 2004, vol. 44, no. 11, p. 1945–1951.
7) Sato, K. et al. KENBIKYO. 2005, vol. 40, No. 3, p. 183–187
8) A. T. Davenport et al. Met. Sci. J. 1968, no. 2, p. 104.
9) Balliger, N. K.; Honeycombe, R. W. K. Metal. Science. 1980, vol. 14, isuue 4, April, p. 121–133.
10) Yamada, K. et al. Proceedings of EMC2008.2008, vol. 2, p. 511–512.
11) Baker, R. G.; Nutting, J. Iron Steel Inst. Special Report, 1959, no. 64, p. 1.
12) Matsuyama, T. et al. Journal of the Japan Institute of Metals and Materials. 1979, vol. 43, no. 7, p. 652–658.
13) D. L. New house ed. Temper Embitterment of Alloy steels. ASTM Special Technical Pub., 1972, p. 499.
14) Boothroyd, C. B. et al. Proceedings of the XIIth International Congress for Electron Microscopy. 1990, p. 80–81.
15) Shigesato, G. et al. Metallurgical & Materials Transactions A. 2014, vol. 45A, p. 1876–1882.
16) Maruyama, N. et al. Shinnittetsu Giho. 2004, vol. 381, p. 31–34.
17) Yamada, K. et al. Proceedings of 52th JSM. 1996, p. 104.
18) Kimoto, K. et al. Journal of Electron Microscopy. 1995, vol. 44, p. 86.
19) Tachibana, S. et al. Corrosion Science. 2015, vol. 99, p. 125–133.
20) Hashimoto, K. et al. Corros. Sci. 1979, vol. 19, p. 3–14.
21) Hamada, E. et al. CAMP-ISIJ. 2009, vol. 22, p. 556.
22) Hamada, E. et al. Corrosion Science. 2010, vol. 52, p. 3851–3854.
23) Ishii, K. et al. JFE Giho. 2008, no. 20, p. 10–15.
24) Ishii, T. et al. Tetsu-to-Hagané. 2011, vol. 97, no. 8, p441–449.